Simulation of polytype formation in zinc sulphide

1990 J. Phys.: Condens. Matter 2 6905

(http://iopscience.iop.org/0953-8984/2/33/003)

J. Phys.: Condens. Matter **2** (1990) 6905–6919. Printed in the UK

Simulation of polytype formation in zinc sulphide

G E Engel
Cavendish Laboratory, Madingley Road, Cambridge CB3 0HE, UK

Received 23 January 1990, in final form 30 April 1990

Abstract. A simple model for the formation of polytypes in ZnS is presented. It is based on theoretically calculated stacking fault energies for this material. Polytypes are explained as metastable structures occurring during the wurtzite–zincblende phase transition. A Monte Carlo simulation of the process results in structures very similar to those observed in experiment. The same mechanism also explains the main features of x-ray data obtained from disordered highly twin-faulted cubic crystals of ZnS.

1. Introduction

ZnS is known to exhibit hundreds of different polytypic crystallographic structures. In an earlier paper (Engel and Needs 1990, hereafter referred to as I), first-principles total energy calculations on five specific structures have been presented. These calculations, though not including finite temperature effects, led to the conclusion that all possible ZnS polytypes are actually very close in structural energy. This helps to answer the question of how ZnS differs from other materials which do not show polytypism: the basic requirement for polytypism is that all the observed polytypic structures have to be nearly degenerate in energy. In the present paper, I address the problem of how the specific structures observed might be formed during the phase transition from the hexagonal to the cubic phase and why some polytypes are less likely to be formed than others.

In order to describe the polytypic structures, a spin notation will be used where the 'spins' s_i take the values $+1$ or -1 (also written as '$\uparrow$' or '$\downarrow$') depending on the way one hexagonal layer is stacked on top of the preceding one (see figure 1 of I). Two parallel spins represent a cubic stacking arrangement and antiparallel spins a hexagonal stacking arrangement. In the Zhdanov (1945) notation, the sequences of spin symbols are further simplified by transforming them into sequences of numbers denoting the widths of bands of parallel spins within a repeat unit of the polytype. The hexagonal structure $(\ldots \uparrow \downarrow \uparrow \downarrow \uparrow \downarrow \uparrow \downarrow \ldots)$ is then written as $\langle 1 \rangle$, the cubic $(\ldots \uparrow \uparrow \uparrow \uparrow \uparrow \uparrow \ldots)$ as $\langle \infty \rangle$ and the structure $(\ldots \uparrow \uparrow \uparrow \downarrow \downarrow \downarrow \ldots)$ as $\langle 3 \rangle$.

In terms of this spin representation, the total free energy of all possible ZnS polytypes can be accurately described by an expression of the form (I)

$$F = E_0(T) - \sum_r J_r(T) \left(\sum_i s_i s_{i+r} \right) \tag{1}$$

where the J_r are temperature-dependent effective inter-layer interaction parameters. J_1

0953-8984/90/336905 + 15 $03.50

is positive and stabilises the cubic $\langle\infty\rangle$ structure at 0 K. J_2 was calculated as being negative and extremely small compared to J_1. All longer-ranged interactions J_3, etc are negligible at $T = 0$.

The dynamical model for the transformation of a 'hexagonal' spin arrangement ($\ldots\uparrow\downarrow\uparrow\downarrow\uparrow\downarrow\uparrow\downarrow\ldots$) to the energetically more favourable polytypes investigated in the present paper has some features in common with an earlier qualitative model (Mardix 1986). It assumes that the transformation proceeds via a single atomic process, namely the successive reversal of single spins from 'up' to 'down' or vice versa, leaving all the other spins in the sequence unchanged. As we will see, this restriction to a single atomic process ensures that the spin sequence, rather than completely transforming to the $\langle\infty\rangle$ phase, ends up in a metastable polytypic structure. In terms of the actual sequence of ZnS layers, spin reversal corresponds to slipping one part of the crystal with respect to the other along a basal plane perpendicular to the hexagonal axis. This type of fault is often called a 'deformation fault'. The model assumes that these faults are introduced into the structures at random locations, but that the probability of their occurrence is related to their stacking fault energy, which varies according to the orientation of the layers in the vicinity of the fault. In addition, the nth spin in the spin sequence is topologically linked to the $(n + N)$th and the $(n - N)$th spin. In the crystal, this corresponds to the presence of a screw dislocation (SD) with Burgers vector N in units of the layer separation. In the true three-dimensional geometry of the crystal containing such a SD, the basal planes are in fact helices with step height N, and layers with a separation N are therefore connected. This connection is responsible for the periodicity of the resulting structures. In a projection of this 3D geometry onto a one-dimensional spin sequence it is simulated by a topological link between spins. In the final version of the model we also allow for different velocities of faults propagating along these links (around the screw). The model is devised to simulate the partial transformations taking place when a ZnS crystal whisker containing a single giant SD of step height N is cooled down from its temperature of growth of around 1700 K to room temperature. The structures obtained from simulations using this model and the statistical distribution of their Zhdanov numbers are remarkably similar to those observed in experiment (Mardix 1986) (sections 4 and 5), and the model is also consistent with x-ray data from randomly disordered cubic crystals obtained by annealing hexagonal crystals (Sebastian and Krishna 1984) (section 3).

2. The basic transformation mechanism

The idea of modelling the transition from the hexagonal phase to less-ordered polytypes by a dynamical process based on inter-layer interaction parameters is not new. For example, Kabra and Pandey (1988) investigated the transition from $\langle 1\rangle$ to a disordered phase in SiC, choosing interaction parameters J_1, J_2 and J_3 such that $J_2/J_1 = J_3/J_1 = -\frac{1}{2}$. With this choice of parameters, the $\langle 3\rangle$ phase is the thermodynamically stable configuration (Selke *et al* 1985), and it is not surprising that the resulting disordered structures contain many 3-bands.

The present model for the spontaneous ordering of a 'hexagonal' spin arrangement towards disordered or polytypic phases when quenched into the stability range of the cubic $\langle\infty\rangle$ phase is based on the following simple rules:

(i) The interaction parameters at the effective transition temperature, which is the temperature where the rate of transformation has its maximum and which is well below

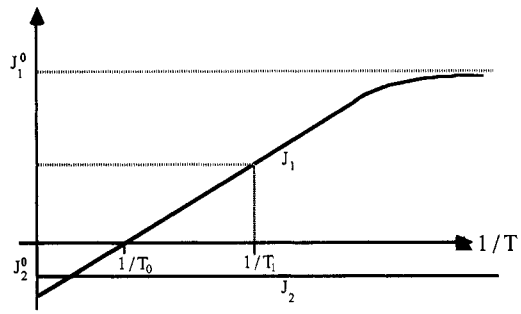

Figure 1. Assumed temperature dependence of the inter-layer interaction parameters J_1 and J_2. At T_0, the ⟨1⟩ phase becomes unstable, which is reflected by a change in the sign of J_1. The parameters of the simulation correspond to T_1, which is the temperature where the rate of transition has its maximum. At $T = 0$, the parameters have the value calculated in I.

the temperature of growth, show the same qualitative behaviour as those calculated for ZnS at $T = 0$, with the interaction J_1 being positive and dominant and with a small negative J_2. All longer-ranged interactions are neglected.

(ii) The atomic process for the transformation is the reversal of a single spin.

(iii) The probability of introducing a stacking fault at a particular position in the spin sequence is related to the stacking fault energy for this particular fault, such that a larger energy gain results in a higher probability for the fault. With only next-nearest-neighbour interactions being significant, the following transformations have to be distinguished:

$$(1)\ldots\downarrow\uparrow\downarrow\uparrow\downarrow\ldots\rightarrow\ldots\downarrow\uparrow\uparrow\uparrow\downarrow\ldots \qquad \Delta E = -(2J_1 + 2|J_2|)$$
$$(2)\ldots\downarrow\uparrow\downarrow\uparrow\uparrow\ldots\rightarrow\ldots\downarrow\uparrow\uparrow\uparrow\uparrow\ldots \qquad \Delta E = -2J_1$$
$$(3)\ldots\uparrow\uparrow\downarrow\uparrow\uparrow\ldots\rightarrow\ldots\uparrow\uparrow\uparrow\uparrow\uparrow\ldots \qquad \Delta E = -(2J_1 - 2|J_2|)$$
$$(4)\ldots\downarrow\downarrow\downarrow\uparrow\downarrow\ldots\rightarrow\ldots\downarrow\downarrow\uparrow\uparrow\downarrow\ldots \qquad \Delta E = -2|J_2|$$

All other transformations do not reduce the energy of the structure and are therefore forbidden. Because $J_1 \gg J_2$, I will distinguish between two groups of faults only. The first group, which I call *fast faults*, includes faults 1, 2 and 3. These faults reduce the hexagonality h of the structure, defined to be the ratio of the number of antiparallel spins with respect to the total number of spins. As antiparallel spins have a large positive energy due to the positive value of J_1, a fault reducing the number of antiparallel spins provides a comparatively large energy gain proportional to J_1. Fault 4, which I call a *slow fault*, does not change the hexagonality of the structure, but the second-nearest-neighbour interaction provides a small energy gain of the order of magnitude of J_2. Forbidden faults will be referred to as *no faults*. Because of the different stacking fault energies for the three types of fault, we expect their introduction to occur at different rates, which explains the terminology.

I now address the above rules in more detail:

(i) As mentioned above, the total energy calculations on ZnS polytypes yield the inter-layer interaction parameters for $T = 0$ only. Not much is known about their behaviour at finite temperatures. The temperature dependence arises mainly from the phonon contribution to the free energies. For SiC, it has been shown by Cheng *et al* (1990) that the differences in phonon frequencies for different polytypic structures result in a small, but significant change in the values of J_r at high temperatures. A similar investigation for ZnS has yet to be carried out. All we can say is that at high temperatures the interactions must be such that the hexagonal phase ⟨1⟩ becomes the stable modification, which indicates that the phonon contribution to the free energy changes the sign of J_1 somewhere beneath the transition temperature of about 1400 K (figure 1). The

present choice of parameters is based on the assumption that the rate of transformation reaches its maximum at a temperature which is significantly below the temperature where $\langle 1 \rangle$ and $\langle \infty \rangle$ are truly degenerate. This is plausible since there may well be a certain energy barrier for the movement of a stacking fault which cannot be overcome unless the energy gain from the structural change is sufficiently large. At the point where this is the case, it is assumed that the ratio $J_1/|J_2|$ has become almost temperature independent and large compared to 1.

(ii) The experimental evidence for this assumption comes from optical investigations on thin crystal whiskers containing a giant SD. It was found that originally straight whiskers start to develop kinks as soon as the temperature is lowered below the transition temperature, and that the kink angles observed are consistent with a mechanism where single deformation faults run around the SD (Mardix *et al* 1968). Recent work on disordered cubic crystals of ZnS (Sebastian and Krishna 1984, Pandey and Lele 1986) also suggests that the transformation mainly proceeds via the introduction of deformation faults.

(iii) This is the most important modification of the simple simulation by Kabra and Pandey (1988). It will be justified mainly by the success of the model. The assumption is plausible due to the different stacking fault energies for fast and slow faults.

3. Monte Carlo simulation of the $\langle 1 \rangle$ to $\langle \infty \rangle$ transformation

In order to test assumptions (i)–(iii) and to calculate an estimate for the probabilities of occurrence α_0 and β_0 for fast and slow faults respectively, a Monte Carlo simulation similar to the study by Kabra and Pandey (1988), but with a different choice of parameters J_1 and J_2 and the distinction between the two types of fault, was performed. The resulting structures show no periodicity because no SD is present. The case with SDs present will be studied in the following sections.

An array of antiparallel Ising spins corresponding to the initial hexagonal configuration is quenched to the stability range of $\langle \infty \rangle$. We assume that at the effective temperature of transition, we are well within the stability range of $\langle \infty \rangle$, hence $J_1 \gg |J_2|$. At each time step, a random position in the spin sequence is chosen and the corresponding spin is flipped with probabilities α_0, β_0 and 0 depending on whether the respective fault is a fast, slow or no fault. The simulation is repeated for various values of β_0/α_0 ranging between 0 and 1. Each simulation, performed on an array of 2000 spins, is run until no further energy gain from a single atomic process can be achieved, yielding a frozen-in metastable structure consisting of small domains of parallel spins. In the usual crystallographic terminology, the fault between two adjacent cubic domains of opposite spin orientation corresponds to a twin fault, and the resulting structure can be described as a highly twin-faulted disordered cubic structure.

In order to allow comparison with experimental data, it is desirable to know the diffraction pattern of an arbitrary layer-sequence. Transforming the spin sequence into the conventional ABC notation for close-packed structures and calculating pair-correlation functions $P(m)$, $Q(m)$ and $R(m)$ of finding the $(n + m)$th layer in stacking position A, B or C respectively if the nth layer is in position A, it is possible to deduce theoretically the diffracted intensity from a stack of N layers along the $(10L)$ direction

of a three-layered hexagonal cell. The intensity I is given by (Holloway and Klamkin 1969)

$$I(L) = N + 2\sum_{m=1}^{N-1}(N-m)(J_m^{(1)}\cos(m\Phi) - J_m^{(2)}\sin(m\Phi)) \tag{2}$$

where

$$J_m^{(1)} = P(m) - \tfrac{1}{2}(Q(m)+R(m)) \qquad J_m^{(2)} = (\sqrt{3}/2)(R(m)-Q(m)) \qquad \Phi = (2\pi/3)L.$$

Instead of having only one atom in the basis, as assumed in the derivation of (2), there are two different types of atom present in ZnS. For the special case where the scattering vector $\boldsymbol{K}$ points in the $(10L)$ direction, the intensity has to be multiplied by an L-dependent factor

$$S(L) = f_{Zn}(L)^2 + f_S(L)^2 + 2f_{Zn}(L)f_S(L)\cos(\pi L/2) \tag{3}$$

where f_{Zn} and f_S are the atomic form factors for Zn and S respectively. Their values and dependence on the scattering angle are taken from Macgillavry and Rieck (1962). The resulting intensity distribution for $\beta_0 = 0$, 0.1 and 0.3 is shown in figure 2(a), whereas figure 2(b) shows the same distribution with the diffraction pattern of a randomly faulted 2H ($\langle 1\rangle$) crystal being superimposed. The latter was obtained by finishing the simulation at a point where only 25% of all possible faults were inserted. As is expected from the theory of diffraction from randomly twin-faulted cubic crystals (Warren 1969), the peaks corresponding to the $\langle\infty\rangle$ structure are broadened asymmetrically and show negligible peak shifts. Comparison with x-ray data (Sebastian and Krishna 1984) shows good agreement both in width and intensity of the main peaks. The appearance of enhanced intensity at positions corresponding to the 6H ($\langle 3\rangle$) structure is seen to be solely due to the special mechanism of stacking fault insertion, which effectively favours the insertion of faults at 2-layer separation. No additional mechanism favouring the insertion of faults preferentially at 3-layer separation is needed to explain this feature. Figure 2(b) also shows that the enhanced intensity at 2H positions found in some of the specimens investigated experimentally can be explained by assuming that the transformation proceeds at different speeds in different parts of the crystal, making the transformation in one part less complete than in the other.

The hexagonality in the case $\beta_0 = 0$, calculated to be $h = 0.135$, is reflected by a broadening of the 3C ($\langle\infty\rangle$) peaks to a half width $\delta = 0.113$ in units of L. The latter is in good agreement with experimental half-widths reported for specimens obtained from annealing hexagonal crystals (Sebastian and Krishna 1984). However, applying the formula used by the authors of that reference to relate h and δ, one would deduce a value $h = 0.106$ from the peak broadening, which is slightly smaller than the exact value, probably because the formula becomes inaccurate at the high fault concentrations encountered in these specimens. For example, cubic domains of width 3 (corresponding to $h = \frac{1}{3}$) do not contribute to the peak broadening, but show up as separate (6H) peaks in the intensity distribution. This is important, because a significantly smaller value of h in real specimens would cast doubt on the purely random nature of the stacking fault insertion. One would have to assume, as has been suggested, by Pandey and Lele (1986), that there are correlations between faults, making it more likely that after initial random insertion of a fault a second fault occurs in the vicinity of the first one, which leads to the growth of the cubic nuclei. As already pointed out in I, the short range of the inter-layer interaction parameters J_r makes such a growth mechanism unlikely in the absence of

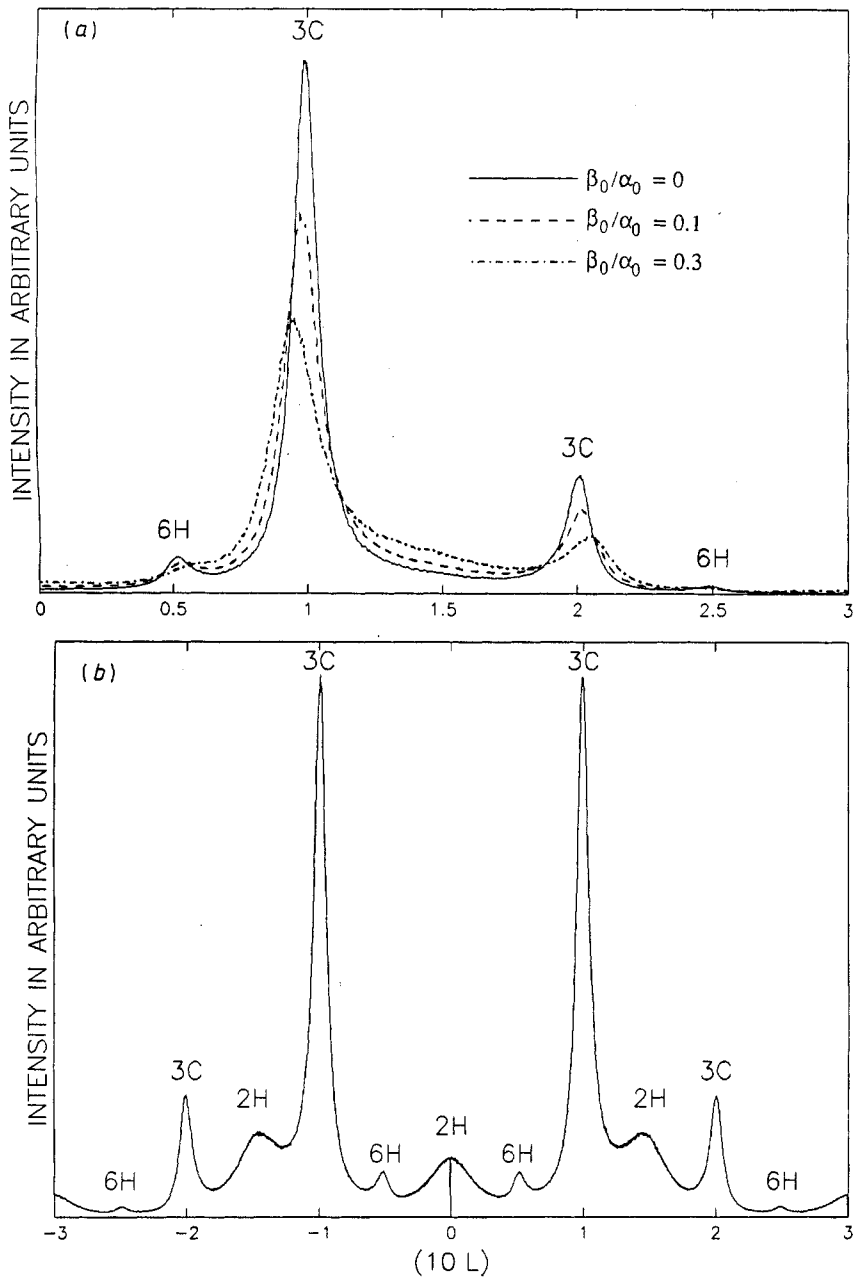

Figure 2. (*a*) Calculated intensity along the (10 *L*) direction of a three-layered hexagonal cell of a disordered highly twin-faulted cubic ZnS crystal obtained from simulated annealing of a 2H crystal for three different values of β_0/α_0. (*b*) Intensity for $\beta_0 = 0$ combined with the diffraction pattern of a faulted hexagonal crystal (25% faulting).

external stresses: it is energetically no more favourable to activate thermally a fault two layers away from another fault than anywhere else. This assumption is corroborated by the agreement between the simulated and experimental diffraction patterns. Exceptions

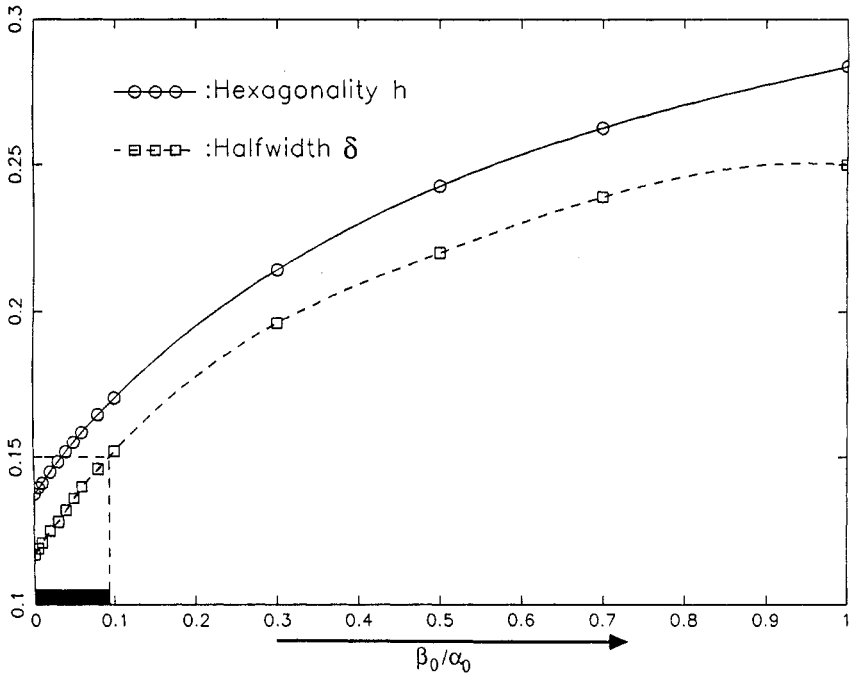

Figure 3. Hexagonality h and halfwidths δ of the 3C peaks in the diffraction pattern along (10 L) diffuse streaks obtained from simulated annealing of a 2H structure as a function of the ratio of fault probabilities β_0/α_0. The range of parameters best reproducing the experimental peak broadening is indicated.

seem to be possible: for example, in some of the specimens investigated by Sebastian and Krishna (1984), δ was less than 0.113, the value found in the simulation for $\beta_0 = 0$, indicating some correlations between faults. In the following, I will neglect these cases.

In order to estimate an upper bound for the probability β_0 of slow faults, figure 3 shows h and δ as a function of β_0/α_0. In the experiments, δ is between 0.08 and 0.15 yielding

$$0 < \beta_0/\alpha_0 < 0.1. \tag{4}$$

4. Transformation mechanism in the presence of a giant SD

In the case where the crystal contains a giant SD (as is found in most specimens containing polytypes) the transformation, rather than leading to a disordered twinned cubic phase, leads to a regular layer sequence whose periodicity is determined by the length of the Burgers vector of the dislocation. Most polytypes are found in thin vapour-grown crystal whiskers, where there is overwhelming experimental evidence in favour of a periodic slip mechanism operating. The mechanism, described in detail by Alexander *et al* (1970), assumes that at some stage during the transformation stacking faults are introduced into the originally hexagonal whisker, either thermally or as a result of external or internal stresses. As soon as the temperature is sufficiently low to provide the negative stacking fault energy needed for the propagation of the faults, they start expanding along the

Table 1. Average bandwidth $1/h$ of ZnS polytypes as a function of the number of layers per unit cell N. The first column shows the values calculated from Mardix's (1986) experimental list, columns 2 and 3 the values obtained from simulations as described in sections 4 ($\beta/\alpha = 0.18$) and 5 ($v_a/v_b = 0.25$, $\beta_0 = 0$, $t_1 = 100\,t_0/N$) respectively. Polytypes containing 1s are not included in the list.

Bandwidth $1/h$				Bandwidth $1/h$				Bandwidth $1/h$			
N	Exp	Sim 1	Sim 2	N	Exp	Sim 1	Sim 2	N	Exp	Sim 1	Sim 2
2	—	—	—	16	4.73	4.73	4.95	30	5.63	7.50	11.25
4	2.00	2.00	2.00	18	4.62	5.03	5.52	32	7.11	4.92	5.33
6	3.00	3.00	3.00	20	4.75	5.09	4.83	34	6.80	6.80	4.86
8	4.00	4.00	4.00	22	5.87	6.77	7.33	36	6.43	6.00	5.29
10	3.75	3.75	3.75	24	4.92	5.37	5.59	38	9.50	4.75	5.43
12	4.15	4.15	4.15	26	4.93	5.96	5.96	40	6.67	5.00	4.44
14	4.67	4.38	4.67	28	6.00	5.60	4.94	44	14.7	4.89	5.50

Total average: Exp: 5.08; Sim 1: 5.03; Sim 2: 5.07.

helical basal planes formed by the giant SD at the axis of the whisker. At the end of the process, stacking faults have been inserted periodically into the structure, the period being determined by the Burgers vector of the SD.

Applying the simple rules of section 2 to small sequences of N spins where the Nth spin is joined to the first spin yields polytypes which are in remarkable agreement with the experimentally observed structures. It is straightforward to produce a list of theoretical polytypes similar to Mardix's (1986) experimental list. For each N ($N = 4, \ldots, 44$), 300 polytypes are created by a Monte Carlo process as in section 3, and if $j(N)$ is the number of experimentally observed polytypes of a given periodicity N, then the $j(N)$ most frequently resulting polytypes of that length are included in the list. The process, of course, completely eradicates all 1s in the Zhdanov sequences, whereas 12 out of 194 experimentally observed polytypes contain one or more 1s. 1s can, in principle, be created by finishing the simulation after a finite number of steps, which corresponds to rapidly cooling down the crystals in a real experiment. For the quantitative analysis, the polytypes containing 1s were not included into the experimental list because their creation in a simulation could be arbitrarily tuned by the number of steps allowed until finishing the simulation. The table of simulated polytypes is compared to the experimental one first by comparing the average hexagonality of each class N of polytypes (table 1) and second by counting the total number of occurrence $g(k)$ of any given Zhdanov number k ($k = 2, \ldots, 40$) in both the simulated and experimental lists (table 2). The only parameter going into the simulation is the ratio β/α. A smaller value decreases the average hexagonality and increases the number of odd Zhdanov numbers (for $\beta = 0$, no even numbers are produced at all), a larger value increases the hexagonality and decreases the odd Zhdanov values. By trial and error, the best agreement with experiment was found for $\beta/\alpha = 0.18$, but the results are still in fairly good agreement for $0.17 < \beta/\alpha < 0.20$. The first column of table 1 lists the average hexagonality of experimentally observed polytypes of a given repeat unit N calculated from the list of currently identified polytypes given by Mardix (1986). For large N ($N > 28$), the values are not very meaningful because of the small number of samples in each class. Also, a few of these long-period polytypes consist of a small number of very large bands of

Table 2. Frequency of occurrence $g(k)$ of Zhdanov numbers $k = 2, \ldots, 44$ from the experimental list of polytypes (Mardix 1986, row 1) and from simulations as described in sections 4 and 5 (Sim 1 and Sim 2 respectively).

k	3	5	7	9	11	13	15	17	19	21	23	25	27	29	31	33	35	37	39	n_{odd}
n_{exp}	203	123	60	24	13	10	3	9	0	3	2	1	0	2	1	0	1	1	0	456
n_{Sim1}	211	98	75	39	19	14	8	6	3	4	0	0	0	1	0	0	0	0	0	478
n_{Sim2}	204	92	56	39	19	15	8	9	2	3	2	0	1	0	0	0	0	0	0	450

k	2	4	6	8	10	12	14	16	18	20	22	24	26	28	30	32	34	36	38	40	n_{even}
n_{exp}	142	66	35	25	9	3	4	1	3	1	1	0	1	0	0	0	1	0	0	0	292
n_{Sim1}	159	44	29	18	13	3	4	2	1	1	2	0	0	0	0	0	0	0	0	0	276
n_{Sim2}	176	35	36	18	13	9	6	2	2	0	1	0	0	0	0	0	0	0	0	0	298

parallel spins only, which indicates that the insertion of faults in the corresponding samples was not completely uncorrelated. Instead, some mechanism inducing the simultaneous introduction of a number of neighbouring faults might have operated in these crystals. Neglecting these cases, we find the average hexagonality of the structures to level off between 17 and 20 per cent as N is increased. From figure 3, we find that this corresponds to a probability ratio $0.1 < \beta/\alpha < 0.2$ for slow and fast faults, which is in agreement with the value chosen for the simulation which gives the best results. Note that in the presence of a SD α and β differ from the probabilities α_0 and β_0 of initial insertion of faults of either type (see below), hence there is no disagreement to the results of the previous section.

5. A more realistic model

In order to gain a deeper understanding of the statistics governing the insertion of faults into a crystal and to explain why the extremely simple model given in the last section accounts so well for the distribution of Zhdanov numbers in the observed polytypes, I will discuss a more realistic model of the phase transition. The model has the following main features:

(i) As before, the crystal is represented by a spin sequence with a topological link between the nth and the $(n - N)$th and $(n + N)$th spins meant to simulate a SD with a step height of N layers.

(ii) Fast and slow faults are randomly inserted into the spin sequence with probabilities α_0 and β_0. The faults dissociate into two partials moving into opposite directions along the topological links, as specified in (iii).

(iii) A fault at position n causes the subsequent introduction of a fault at position $n + N$ (or $n - N$, depending on the direction of the fault propagation) after a time t_0 which is inversely proportional to the fault velocity. Hence the faults propagate along the topological links, which corresponds to the movement of Shockley partials along the helical basal planes provided by the SD. The velocities of fast and slow faults are v_a and v_b respectively, where $v_a > v_b$.

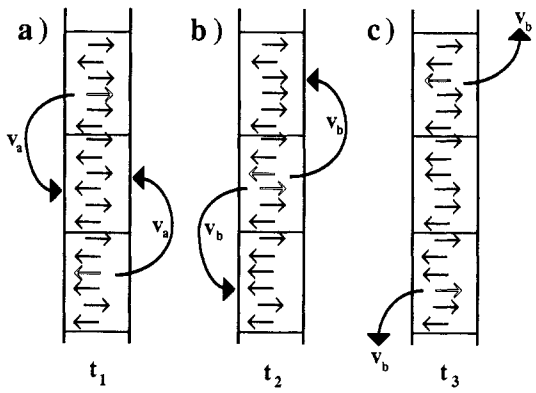

Figure 4. Schematic drawing of the interaction between two deformation faults moving along the spin sequence in opposite directions on neighbouring layers. As the faults meet, their stacking fault energy change, reducing their velocity from v_a to v_b.

(iv) If faults moving into opposite directions meet on the same or on neighbouring planes, it can easily be seen (figure 4) that their stacking fault energy becomes less negative or even positive. A less negative stacking fault energy causes the fault to move at a smaller velocity. An example for this is given in figure 4: two fast faults are effectively converted into slow faults. A positive stacking fault energy stops the movement completely.

We consider an arbitrary subsequence of N spins within the spin chain, where N is the periodicity of the polytypes, and determine the probability of a fault occurring at a particular position within this sub-sequence. For this purpose, we average over a large ensemble of similar spin chains containing this particular sub-sequence. Clearly, positions in the sub-sequence where introduction of a fault causes the same change in structural energy have equal fault probabilities. Again, we distinguish between positions where the energy change is proportional to J_2 and J_1 respectively. Without loss of generality, we can reduce the problem to finding the probability ratio β/α of introducing a fault at positions 3 or 4 in the sequence ($\uparrow\uparrow\uparrow\downarrow\uparrow$). This ratio should be time dependent since there are two time-scales in the simulation: the time between insertion of two faults and the inverse fault velocity, which in a real transformation process are also likely to vary independently with temperature. We consider two limiting cases:

(a) At the beginning of the process, the probability is simply given by the probability of initial insertion of a fault (see section 3):

$$\beta/\alpha = \beta_0/\alpha_0 \qquad (t \to 0). \tag{5}$$

(b) At a later stage of the transformation, initial creation of new faults becomes increasingly unlikely, as the number of untransformed spins decreases. Instead, we have a large number of moving faults. Consider the fault on position 2 of the sequence ($\uparrow\uparrow\uparrow\downarrow\uparrow$). This fault moves along the whisker until it interacts with a fault moving in the opposite direction. In a long whisker containing many faults, it is equally likely that this fault is in either of the positions 3 or 4. Hence, it is equally likely to have a fault occurring in either of these positions within the transformed region. Now, we consider the combined flux of faults of a certain type through many similar specimens forming the ensemble. This depends not only on the number of faults of either type (which should be equal on average), but also on their velocity. Hence, as faults in position 4 move faster than those in position 3, we find that the total flux of faults in position 4 within the

transformed region is larger than the flux of faults at position 3. Consequently, the ensemble averaged probability of a fault intersecting our sub-sequence on position 3 or 4 is proportional to the fault velocity:

$$\beta/\alpha = v_b/v_a \qquad (t \to \infty). \tag{6}$$

From this qualitative argument, we expect that for general times t, we have the inequality

$$\beta_0/\alpha_0 < \beta/\alpha < v_b/v_a. \tag{7}$$

Replacing β/α by an effective mean value, we get back to the simulation of the previous section. This is the justification of the model presented in the previous section.

A full analysis would also have to consider finite size effects: 'creation' of a fault by interaction with already existing faults (process b) can only occur during the finite time it takes the fault at position 2 to traverse the whole whisker; after that, a fault at position 3 or 4 can be formed only by thermal activation of a new fault on the corresponding position somewhere in the whisker (process a). This size effect should become small if the whisker is long enough to make it certain for every moving fault to encounter another one moving in the opposite direction on neighbour or second-neighbour planes.

Despite these complications, most general features of the model depend only on the choice of β_0/α_0 and v_b/v_a, and the model gives polytypes similar to the experimental ones and those obtained from the previous model (section 4) for a rather wide range of parameters. A simulation of the process was carried out to compare the resulting polytypes with those from section 4 and with experiment. For every N ($N = 4, \ldots, 44$) a spin sequence of $M \times N$ antiparallel spins, where $M = 100$, was relaxed according to rules (i)–(iv) under the following additional assumptions:

(v) following the results of section 3, which suggests that initial insertion of slow faults is extremely unlikely compared with the insertion of fast faults, we set $\beta_0/\alpha_0 = 0$—thermal activation of faults occurs only if the hexagonality of the structure is reduced.

(vi) The thermal activation of initial faults is simulated by the following procedure: at an average rate $1/t_1$ (t_1 being the average time between insertion of faults), a spin is randomly chosen among all spins in the sequence; this spin is flipped if and only if the corresponding fault is a fast fault. The time t_1 is chosen as Mt_0/N, where Mt_0 is the time for a fast fault to move along the whole whisker. This ensures that the insertion probability per unit length of the whisker is constant for varying N and that any given fault is likely to interact with many other faults before reaching the end of the whisker.

The resulting spin sequence is found to be segmented into many regions of varying size mN (m integer), each of which contains a single polytype. Of course, all polytypes from a single simulation belong to the same family N determined by the SD. This segmentation is exactly what is found in experiment (Mardix *et al* 1987). In the present model, a border between two such regions occurs because the interaction of two faults moving in opposite directions changes their energy from negative to positive, thus stopping the movement of both faults.

Repeating the simulation 100 times for each N and choosing randomly a few sub-sequences of length N within each of the resulting structures, these were statistically analysed in exactly the same way as described in section 4. The results for $v_b/v_a = 0.25$ are listed in tables 1 and 2 and show fairly good agreement with both the distributions from section 4 and with experiment; small deviations are easily explained by the small

number of samples available for the statistical analysis of the experiment. Table 3 shows the most frequently resulting polytypes for $N = 4, \ldots, 20$. Similar to what was found for the parameter β/α in section 4, the results depend relatively weakly on changes in v_b/v_a over a wide range. Decreasing the velocity ratio increases the number of odd elements, increasing it increases the even elements. 1s can be created by finishing the simulation after a finite number of steps.

6. Discussion

Given the number of simplifications in the model, it is somewhat surprising that it should give such an accurate description of the statistics of the Zhdanov numbers of ZnS polytypes.

One simplification which could easily be removed by assigning a mean free path to each fault is that the model does not explicitly allow for possible interactions between the moving partials and other types of obstacle like impurities or lattice defects, which in some cases might impede or even stop the propagation of a fault. Experiment, however, shows that faults move along the whisker over considerable distances, making this a minor effect. Another possible complication is that faults might not always remain in the same glide-plane, but that there could be mechanisms by which they change to, say, a neighbouring plane during their propagation.

Furthermore, the ratio of the fault velocities and the rate of initial insertion of faults are certainly temperature and hence time dependent. These parameters may also vary with impurity concentration or pressure. This does not cause too serious a problem as long as the variation in the ratio between them is not too large, because as we have seen the main results of the simulation are relatively insensitive to changes in the parameters.

The model hinges critically on the assumption that the fault velocities depend on the stacking fault energies and that they are small enough to allow interactions between faults which originate from various places in the whisker. The latter assumption seems justified since the partial has to move around a helix with very low step height, making the total path length from one end of the whisker to the other extremely long. Also, the segmented structure of the experimentally observed whiskers indicates that faults in general do not traverse the whole whisker at once.

Normally, in the theory of fault or crack propagation in crystals, one finds a relationship between the crack velocity and the applied external stresses such that a higher stress results in a higher velocity. In our case, this stress is provided by the internal force from the negative stacking fault energy. If the relationship between velocity and stress were linear, we would expect $v_b/v_a = |J_2|/J_1$, the ratio of the stacking fault energies for slow and fast faults. At $T = 0$ K, $|J_2|J_1 = 0.05$ according to I, but probably the value of J_1 near the transition temperature is smaller than the calculated one, bringing the ratio closer to 0.25, which is the velocity ratio giving best agreement with experiment in the simulation. Comparison of the parameter values also shows that equation (7) holds for the values of β_0/α_0, β/α and v_b/v_a quoted in sections 3, 4 and 5 respectively. Actually β/α and v_b/v_a are rather close, indicating that the probability of a fault occurring at a fast or slow fault position is mainly determined by its velocity rather than the probability of initial insertion. This explains the relatively large occurrence of even numbers in the Zhdanov sequence: although faults are initially activated on fast fault positions only, which by itself creates only cubic domains with an odd number of layers, the interaction mechanism of

Table 3. List of the most frequently occurring polytypes found in 100 simulation runs for the model of section 5 with $v_a/v_b = 0.25, \beta_0 = 0, t_1 = 100t_0/N$ and $N = 4, \ldots, 20$. N is the repeat period of the polytypes. An asterisk in front of the Zhdanov number indicates that the corresponding structure or that of a polytype with the same numbers in different order has not yet been found experimentally. The polytype $\langle\infty\rangle$, which is found in all simulations with small Burger vector N, was not included in the statistical analysis of tables 1 and 2, the polytype $\langle 33\rangle$ which is found both for $N = 6$ and $N = 12$ was included only once.

N	Polytype	No of occurrence	N	Polytype	No of occurrence
4	(∞)	198	16	13 3	29
	2 2	102		9 7	28
				*11 5	24
6	(∞)	129		14 2	19
	3 3	95		* 9 3 2 2	17
	4 2	76		10 6	17
				* 8 3 3 2	14
8	5 3	127		7 3 3 3	13
	6 2	80		* 6 3 5 2	12
	(∞)	76		5 5 3 3	11
	4 4	8		7 3 4 2	11
10	8 2	75		(∞)	10
	7 3	67		* 6 5 3 2	9
	(∞)	58		* 7 5 2 2	9
	5 5	38			
	3 3 2 2	23	18	7 5 3 3	23
	6 4	22		15 3	20
	4 2 2 2	11		*11 7	15
				7 3 6 2	12
12	9 3	79		7 3 5 3	11
	7 5	48		13 5	11
	10 2	37		* 9 9	10
	5 3 2 2	32		(∞)	10
	(∞)	31		*16 2	10
	(3 3 3 3)	17		5 5 5 3	10
	6 6	13		*11 3 2 2	8
	4 3 3 2	12		8 5 3 2	8
	8 4	10		*12 6	6
	4 4 2 2	7		* 9 5 2 2	6
	6 2 2 2	5		10 8	6
				9 3 4 2	6
14	12 2	41		7 6 3 2	5
	9 5	36		9 4 2 3	5
	(∞)	33		* 8 6 2 2	5
	7 7	30		* 6 2 3 3 2 2	5
	11 3	27			
	5 3 3 3	18	20	7 7 3 3	11
	* 7 3 2 2	17		*11 3 3 3	11
	5 3 4 2	15		17 3	11
	* 6 3 3 2	15		*15 5	11
	*10 4	11		* 7 6 2 5	10
	5 4 2 3	10		—	—
	8 6	7		—	—

section 5 ensures that faults can also occur at slow fault positions, resulting in the formation of bands with an even number of layers.

As mentioned in the introduction, an explanation for the statistical distribution of Zhdanov numbers in ZnS polytypes by a model based on the periodic slip mechanism has already been put forward by Mardix (1986). It made various assumptions on the thermodynamic stability of cubic domains of various sizes with temperature and hence, as the latter is not known, does not seem to allow a quantitative analysis. Nevertheless, some of the more qualitative arguments given by Mardix also apply to the present model. For example, the fact that the number of occurrences of a certain Zhdanov number, k, decreases roughly as $g(k) = A(1/2)^{2k}$ (or $g(k) = B(1/2)^{2k+1}$), with separate prefactors A and B for the even and odd numbers respectively, follows simply from the consideration that, given a spin sequence $\langle 3111 \rangle$, it is equally likely that, after the introduction of a fault, one of the sequences $\langle 51 \rangle$ or $\langle 33 \rangle$ is formed. Hence the probability of finding a 5 is half the probability of finding a 3. Also, even numbers are only formed by a special process from configurations like $\langle 31 \rangle$, $\langle 51 \rangle$, ...

The present model has the advantage of allowing a quantitative analysis. It also yields an explanation for the segmentation of whiskers into different polytypic regions, and it is consistent with the transformation mechanism for crystals not containing dislocations (section 3). Furthermore, we now understand why in all experimentally observed polytypes containing 1s all the other numbers have odd values only. These polytypes are formed if the transformation process is frozen in at an early stage. Then ((5)) the fault probability is mainly determined by β_0/α_0, making the occurrence of a slow fault in order to create an even Zhdanov number extremely unlikely.

A crucial test of the model would be to determine the structures of neighbouring regions in a whisker and to see whether they indeed contain faults which are incompatible in the sense that neither of them can proceed in the adjacent region because of a positive stacking fault energy. Of course, there might be some cases when the movement of a fault was simply frozen-in once the temperature became too low, which can also give rise to a border between regions. It would further be interesting to determine experimentally the fault velocity of the two types of fault proposed in this paper. Polytypes containing 1s should be readily obtainable by cooling down the whiskers rapidly. A lot of theoretical work is needed to understand the initial creation and propagation of faults at the atomic level in a covalent–ionic material such as ZnS.

Finally, it should be noted that a few polytypes such as $\langle 50\,4 \rangle$ containing extremely long bands of parallel spins cannot be explained by the proposed model. Their existence indicates that there are experimental situations when the initial insertion of faults does not occur purely at random. Local stress fields might have caused the instantaneous introduction of a number of faults at two-layer separations in these specimens; if these faults propagate round the SD all at once, a polytype with extremely large bands might result.

7. Conclusions

The bewildering variety of polytypic structures found in ZnS, containing bands both with an even and odd number of layers, has been explained as the result of a dynamical process governing the transformation from the hexagonal to the cubic phase in the presence of a giant screw dislocation. The process is driven by the negative stacking fault energies of single deformation faults in this material, and the actual structures result

from the interaction of such faults and their different velocities. In the absence of a SD, the transformation ends up in a metastable disordered cubic phase whose diffraction pattern is similar to those observed experimentally for highly twin-faulted cubic crystals.

Acknowledgments

I would like to thank R J Needs and V Heine for many enlightening discussions. The financial support of the Deutscher Akademischer Austauschdienst is gratefully acknowledged.

References

Alexander E, Kalman Z H, Mardix S and Steinberger I T 1970 *Phil. Mag.* **21** 1237
Cheng C, Heine V and Jones I L 1990 *J. Phys.: Condens. Matter* **2** 5097
Engel G E and Needs R J 1990 *J. Phys.: Condens. Matter* **2** 367
Holloway H and Klamkin M S 1969 *J. Appl. Phys.* **40** 1681
Kabra V K and Pandey D 1988 *Phys. Rev. Lett.* **61** 1493
Macgillavry H and Rieck G D (ed) 1962 *International Tables for X-Ray Crystallography* vol 3 (Birmingham: Kynoch) p 202
Mardix S 1986 *Phys. Rev.* B **33** 8677
Mardix S, Kalman Z H and Steinberger I T 1968 *Acta Crystallogr.* A **24** 464
Mardix S, Lang A R, Kowalski G and Makepeace A P W 1987 *Phil. Mag.* A **56** 251
Pandey D and Lele S 1986 *Acta Metall.* **34** 415
Sebastian M T and Krishna P 1984 *Phil. Mag.* A **49** 809
Selke W, Barreto M and Yeomans J 1985 *J. Phys. C: Solid State Phys.* **18** L393
Warren B E 1969 *X-Ray Diffraction* (New York: Addison-Wesley)
Zhdanov G S 1945 *C.R. Acad. Sci., URSS* **48** 39